ESA Contract Report

SMOS ESL contract 4000130567/20/I-BG

Contract Report to the European Space Agency

Annual SMOS brightness temperature monitoring report - 2023/24

Authors: Kirsti Salonen, Pete Weston and Patricia de Rosnay
Contract officer: Raffaele Crapolicchio

December 2024

Series: ECMWF - ESA Contract Report

A full list of ECMWF Publications can be found on our web site under:

http://www.ecmwf.int/publications/

European Centre for Medium Range Weather Forecasts
Shinfield Park, Reading, RG2 9AX, England

Abbreviations

BUFR ..... Binary Universal Form for the Representation of meteorological data
CMEM ..... Community Microwave Emissivity Modelling platform
ECMWF ..... European Centre for Medium-range Weather Forecasts
ESA ..... European Space Agency
IFS ..... Integrated Forecast System
NRT..... Near Real Time
NWP..... Numerical Weather Prediction
RFI..... Radio Frequency Interference
SMAP ..... Soil Moisture Active Passive
SMOS ..... Soil Moisture and Ocean Salinity
Tb ..... Brightness Temperature

1. Introduction

This document provides an annual summary of the performance of the European Space Agency (ESA) Soil Moisture and Ocean Salinity (SMOS) brightness temperature (Tb) monitoring run routinely at the European Centre for Medium-range Weather Forecasts (ECMWF). The period covered is September 2023 to August 2024. Several different monitoring plots are presented, and notable features are discussed in detail. Also, potential improvements to the monitoring system are proposed.

2. Annual SMOS monitoring results

Routine operational monitoring of SMOS observations from the near real time BUFR (Binary Universal Form for the Representation of meteorological data) product is performed at ECMWF. The SMOS measured brightness temperatures are compared to short-term numerical weather prediction (NWP) forecasts transformed into brightness temperatures using the Community Microwave Emissivity Model (CMEM; de Rosnay et al. 2020). The CMEM outputs are simulated brightness temperatures in the Earth frame, and these are converted into the SMOS antenna frame using the geometric and Faraday rotation angles provided with each observation in the BUFR files. Differences between observations and their model counterparts are known as background departures and statistics of these background departures are accumulated and plotted routinely.

The samples used to produce the plots can be filtered by area, including global, Northern and Southern Hemispheres, as well as loose definitions of the continents: Europe (120°W-120°E, 35°N-77.5°N), Asia (0°W-120°W, 40°N-82.5°N), North America (120°E-0°E, 20°N-77.5°N), South America (120°E-0°E, 40°S-17.5°N) and Australia (0°E-120°W, 47.5°S-7.5°S). This section focuses on global statistics.

The plots are produced separately for data:

- Over sea or over land
- With different incidence angles: 30°, 40° or 50°
- With different polarisations: H (XX) or V (YY) at the SMOS antenna reference frame
- RFI unscreened/screened
- Ascending and descending orbits

A selection of different options for surface type, incidence angles and polarisations are presented, and the full set of plots for the RFI screened data are available via FTP at ftp://dpgswebserver-2.smos.eo.esa.int/SMOS_ESL2021/Task-5/Annual_Monitoring/2024/All_plots_2023_2024.zip).

A thorough introduction to the monitoring system can be found in Salonen et al. (2024b) and examples of the plots produced can be seen at https://www.ecmwf.int/en/forecasts/quality-our-forecasts/monitoring/smos-monitoring, where also monitoring statistics for data without RFI screening are available. In this report the focus is on RFI screened data.

In this section each of the different types of plots produced as part of the SMOS monitoring system are presented and any notable features are highlighted to be investigated in more detail in the following sections.

2.1. Time series

In the time series figures, statistics are plotted as lines against time on the x-axis for the full twelve-month period with statistics accumulated in 12-hour chunks. The statistics plotted are mean and standard deviation of background departures, the mean observed and background brightness temperatures and number of observations. These plots allow global trends and jumps in the statistics to be identified.

Figures 1 and 2 show that the background departure statistics over land are generally very stable over the year. However, there are two gaps in the timeseries, namely 8 – 13 September 2023 and 22nd February – 12th March 2024. These are due to on-board GPS anomaly and SMOS entering safe hold mode, respectively. In addition, 11th August 2024 is excluded from the time series due to strong RFI signal over Alaska. These anomalies are discusses in more details in Section 3. The mean background departures mostly vary between ±5K for H polarisations and ±3K for V polarisations with only very occasional global mean values outside of this range. The standard deviation of background departures has slightly more day-to-day variability but generally stay close to a value of ~17K for H polarisations and ~14 – 15K for V polarisations. Overall, the statistics are very similar compared to the corresponding values from 2022/23 (Salonen et al., 2024a) indicating that SMOS is behaving in a stable way. The apparent slightly better performance of the V polarisations over the H polarisations could be due to an instrument effect but it could also be due to differing performance of the CMEM observation operator used to convert the model soil moisture to brightness temperature. It should be noted that the background departures presented here do not have a bias correction applied and the statistics are consistent with those found between 2010 and 2016 without bias correction in de Rosnay et. al. (2020).

Figure 3 shows that there is mostly less annual variability in the background departure statistics over sea than over land. The number of observations between October 2023 and June 2024 is much more stable over sea due to proportionally smaller areas of ocean covered by sea-ice than snow-covered land areas. Over land time variant factors impacting the soil moisture include also frozen soil. There are few notable spikes in the departure statistics over sea, namely 3rd October 2023, 14th December 2023, 1st January 2024, 13th March – 18th April 2024, 8th May 2024, 13th May 2024 and 11th August 2024. All these except 8th May 2024 are due to short lived RFI sources and are discussed in more details in Section 3.

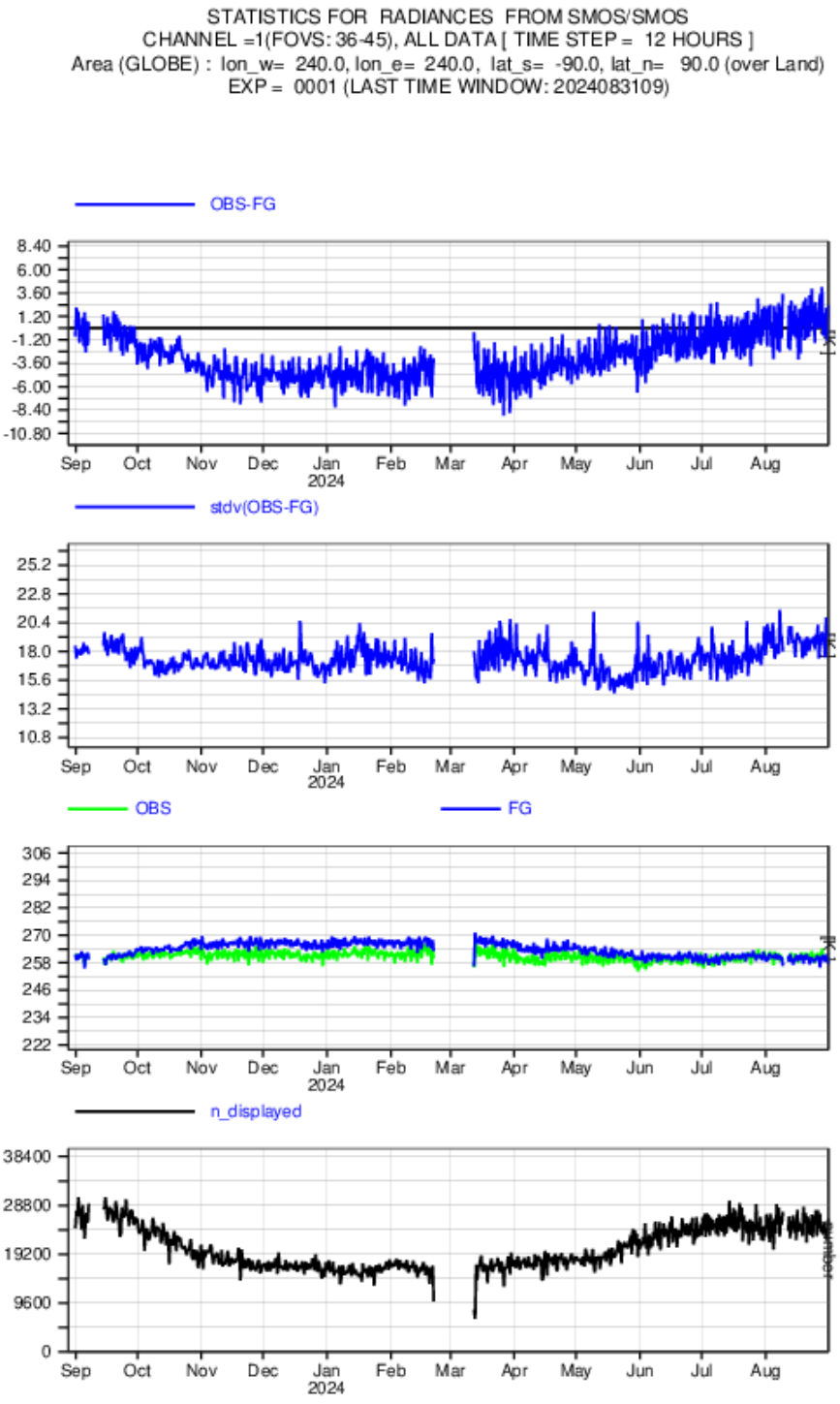

Figure 1: Time series of mean background departures (upper panel), standard deviation of background departures (2nd panel), mean observed and background values (3rd panel) and number of observations (lower panel). Statistics are accumulated into 12-hour bins for SMOS observations over land at 40° incidence angle, H polarisation and cover 1st September 2023 to 31st August 2024.

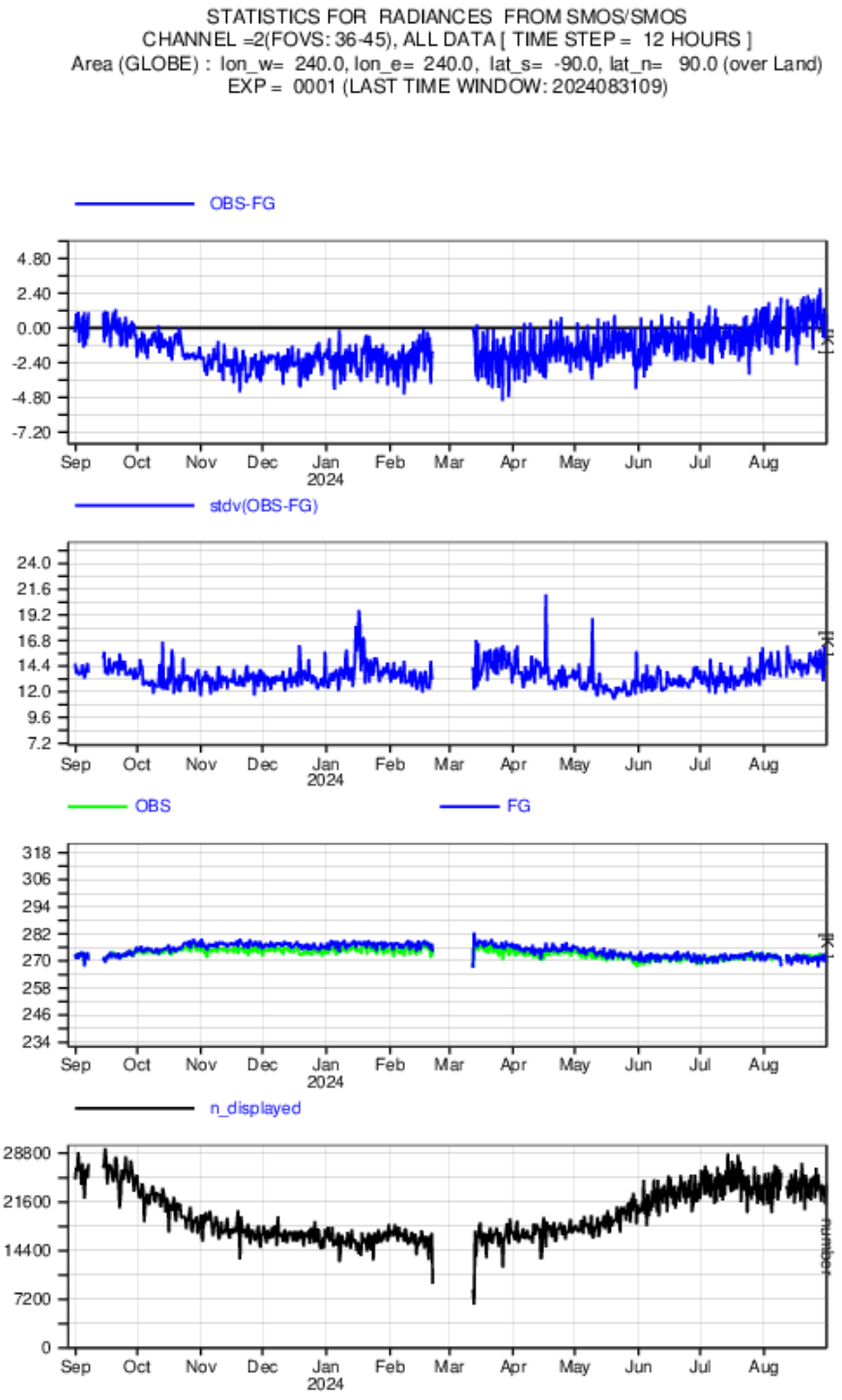

Figure 2: As figure 1 but for SMOS observations with V polarisation

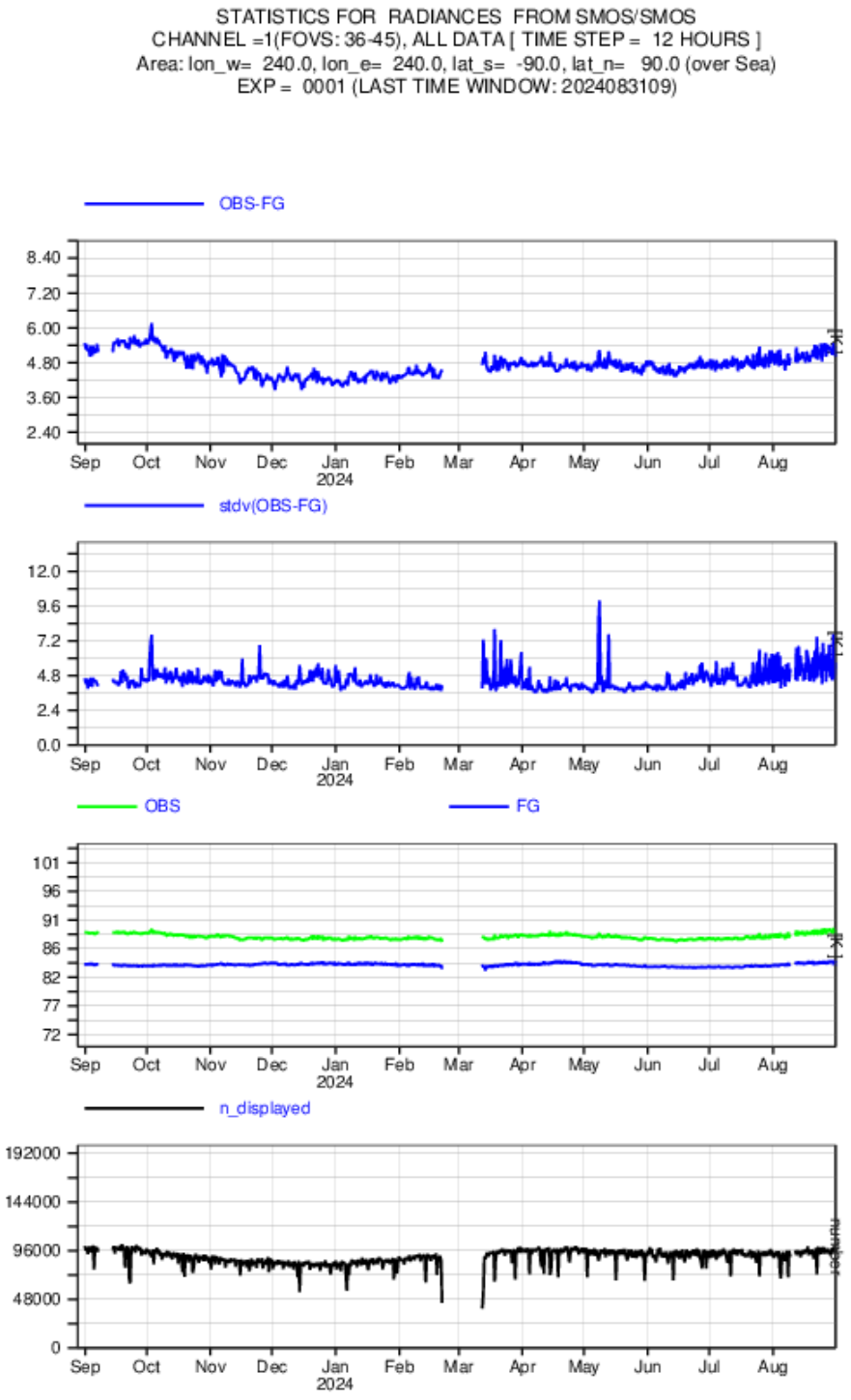

Figure 3: As figure 1 but statistics are accumulated for SMOS observations over sea at 40° incidence angle and H polarisation.

2.2. Hovmöller plots

Statistics presented in this section are plotted as a heat map (Hovmöller plot) with time on the x-axis and latitude on the y- axis for the twelve-month period with statistics accumulated in 2.5° latitude bins and 12-hour chunks. The statistics plotted are mean and standard deviation of background departure, mean and standard deviation of observed value and number of observations. These plots allow local trends and jumps in the statistics to be identified.

Figure 4 shows various seasonal patterns in the variability of the background departures over land for 30° incidence angle and V polarisation as an example of the monitoring results. There are areas of larger standard deviations of background departures at 10-30°N in September and October 2023 and June, July, August 2024 and 10-30°S in January to April 2024. These areas and times of year correspond to the wet season in the tropics and higher variability in model precipitation leading to higher variability in model soil moisture is the likely cause. There is also a large area of increased standard deviations of background departures between 60-80°N which corresponds to an area of positive bias in the background departures over Siberia. This is only visible in the Northern hemisphere (NH) summer because observations over these areas are screened out due to snow cover and frozen ground in NH winter. The feature can also be seen in the gridded maps in section 2.3. Generally, all incident angles and both H and V polarisations show signals of the same features.

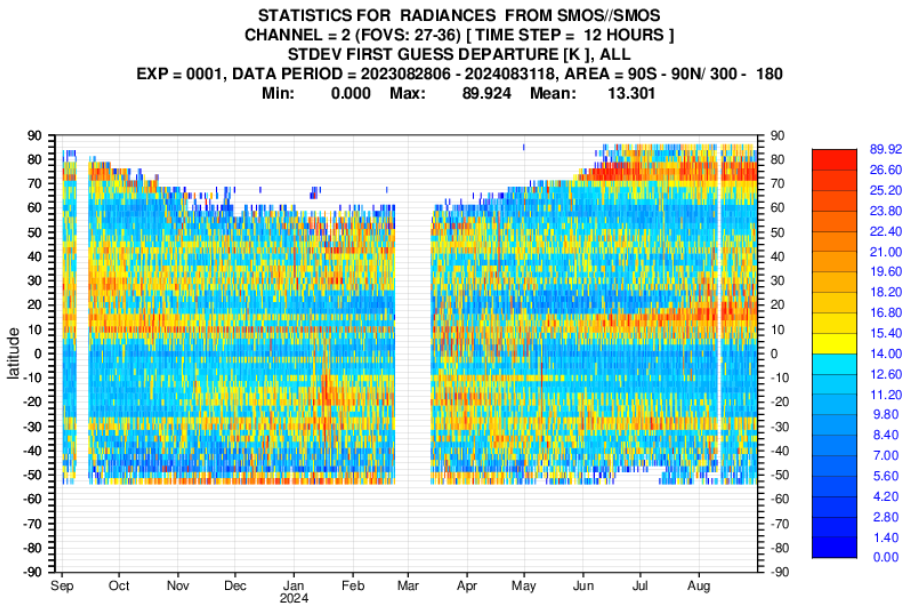

Figure 4: Hovmöller plot showing SMOS background departure standard deviation monitored over land at 30° incidence angle, V polarisation covering 1st September 2023 to 31st August 2024

Figure 5 shows the hovmöller plots for number of observations (top panel), standard deviation of observed values (middle panel) and the background departure standard deviation (lower panel) for incidence angle 30° H polarisation over sea. There are similar features in the statistics occurring from November to February between 0 and 45°N than observed during the same period in 2022-2023 (Salonen et al., 2024a). The number of observations is dropping over Southern hemisphere and the standard deviation both of the observed values and background departures is increasing over the Northern hemisphere. In Salonen et al. (2024a) these anomalies were concluded to be due to solar effect. The 2023-2024 anomaly is discussed in more detail in Section 3.

Other notable features in Fig. 5 include increased values of observation as well as background departure standard deviation on 3rd October 2023 between 15°S - 30°N, 14th December 2023 between 55 - 60°N, 12th March – 18th April between 10°N - 20°N, 8th May 2024 between 60°S and 40°N and 13st May 50°N - 60°N. All these features, except 8th May 2024 (see Section3), are related to short lived RFI sources.

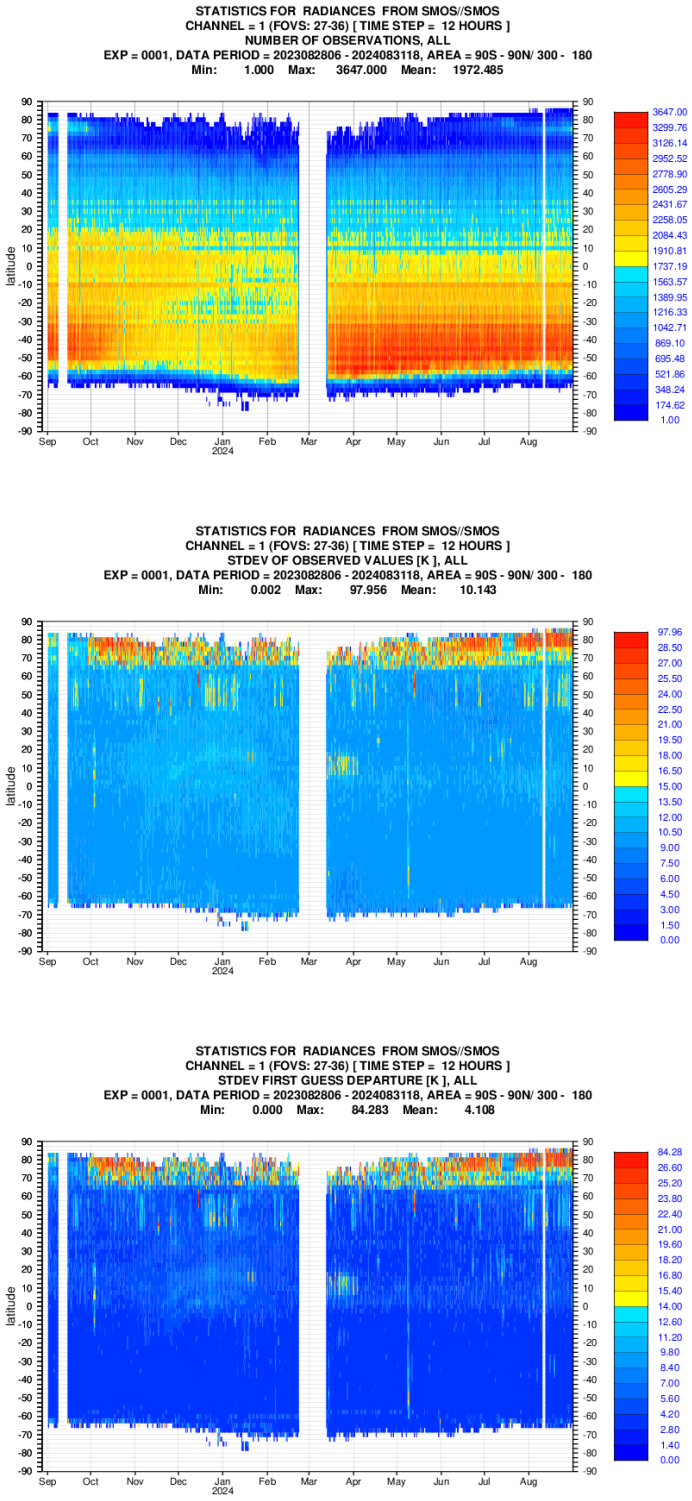

Figure 5: Hovmöller plots showing SMOS number of observations (upper panel), observation standard deviation (middle panel) and background departure standard deviation monitored over sea at H polarisation and 30° incidence angle, respectively. The period covered is 1st September 2023 to 31st August 2024.

2.3. Maps

Figure 6 shows the geographical distribution of biases in the SMOS background departures over land. Figures 1 and 2 indicate relatively small global mean background departures but figure 6 shows that there are areas with significantly large biases. Large positive biases are seen over Europe, Northern and Eastern Asia and South America, while large negative biases are evident over large parts of Africa, South-Western Asia, Australia and the far North of North America. The distribution of biases is very similar than reported for 2022/23 in Salonen et al. (2024a).

Figure 7 shows that the largest variability in background departures remains over the Middle East, central and Eastern Asia, and has significantly increased over Europe compared to 2022/23. This is caused by RFI in those regions with the strength and location of RFI sources varying significantly throughout the year. The RFI situation over Europe is a consequence of the war in Ukraine. The improved v724 RFI screening in use since 2021 has significantly reduced the magnitudes of RFI signal in the statistics, and due to the effective screening large areas over Ukraine and Russia have no data. However, Fig. 7 shows that the screening is still not perfect.

Figure 8 shows the background departure standard deviation over sea for incidence angle 50°, V polarisation. There are areas of increased background departures surrounding the coasts of Europe, in the Mediterranean Sea, the Arctic areas and Asia due to RFI contamination. Compared to 2022/23 (Salonen et al., 2024a) the RFI signals have overall slightly decreased over sea surfaces. However, some of the sources which are more short lived do not appear clearly in the yearly statistics. Over the Northern and Southern polar regions there are slightly increased background departures compared to other regions, due to a combination of smaller sample sizes due to sea-ice screening and slight sub-optimalities in the sea-ice screening during rapid melting and freezing events. Away from the RFI affected and polar regions there is very little variation in background departures due to lower Tb variations over ocean which are mostly caused by temperature variations. In addition, the observation operator CMEM treats the sea surfaces as flat surfaces like lake surfaces. Hence, there is currently no variation in simulated brightness temperature from waves or surface wind-speed as there will be in the observed brightness temperatures.

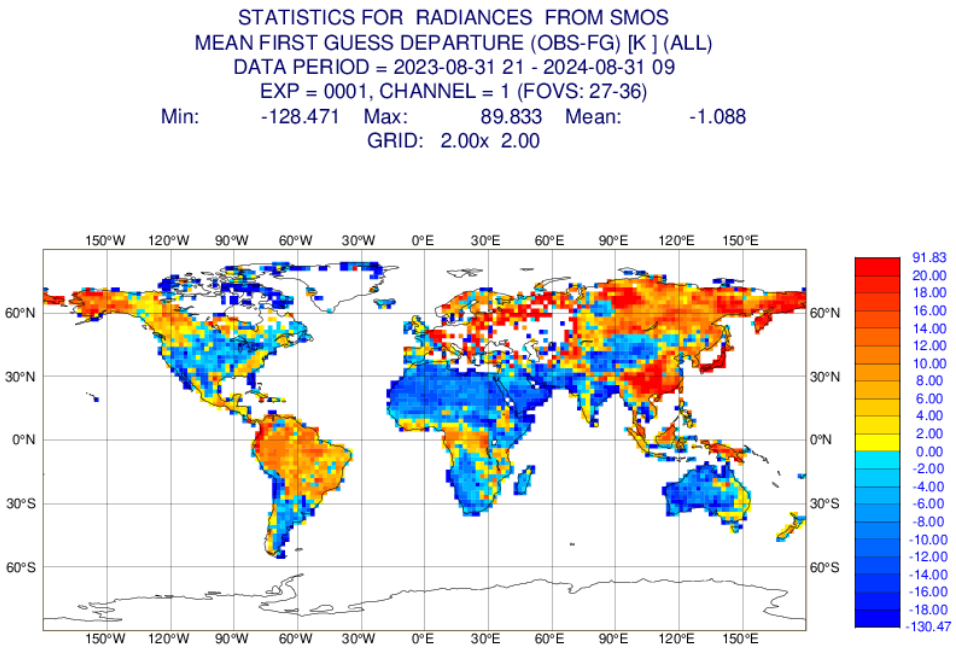

Figure 6: Gridded map plot showing the mean of SMOS background departures over land at 30° incidence angle, H polarisation covering 1st September 2023 to 31st August 2024.

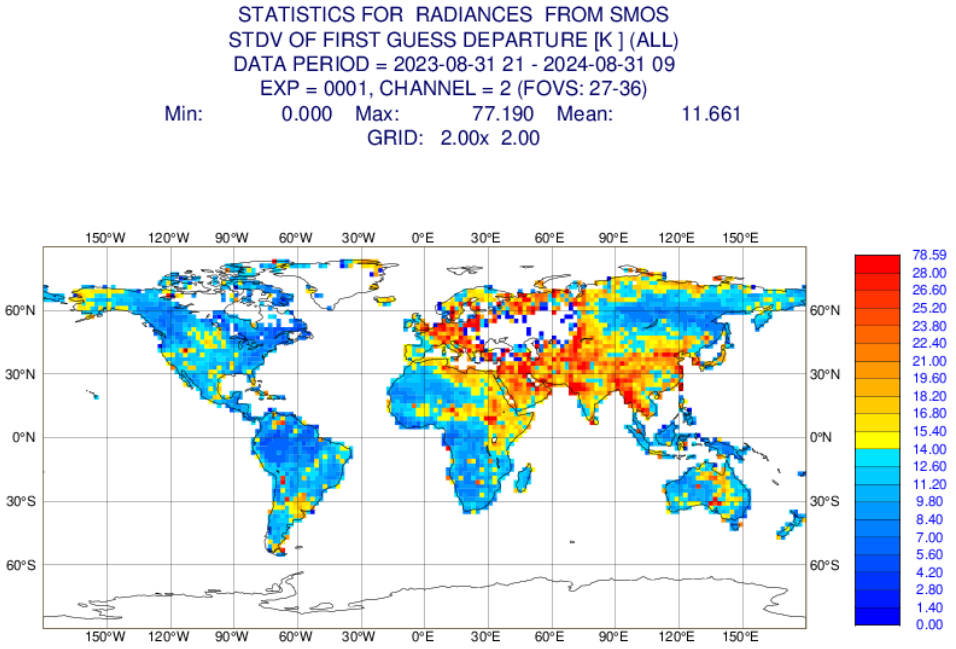

Figure 7: Gridded map plot showing the standard deviation of SMOS background departures over land at 30° incidence angle, V polarisation covering 1st September 2023 to 31st August 2024.

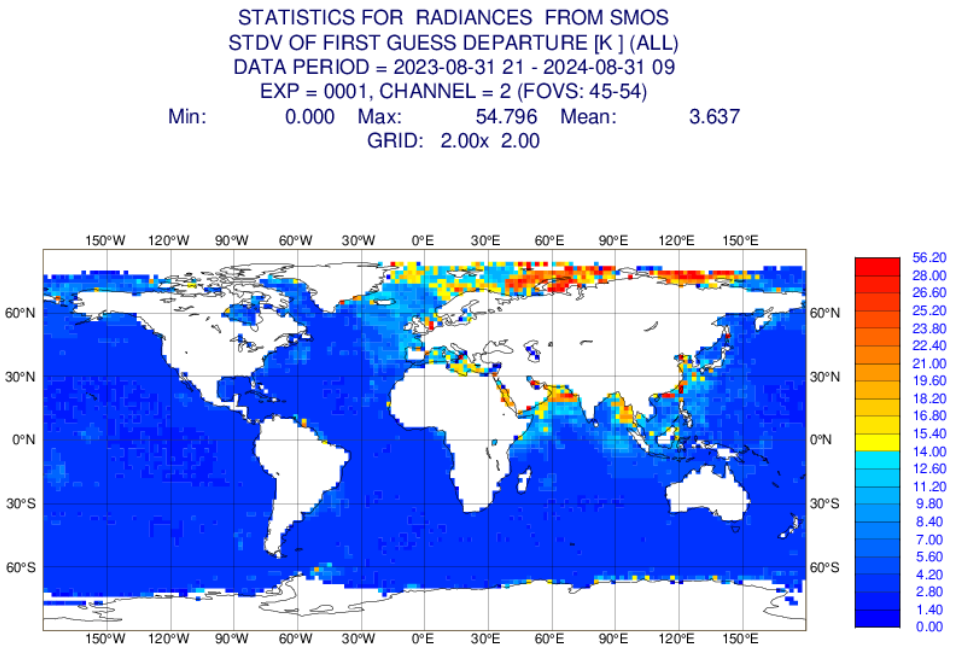

Figure 8: Gridded map plot showing the standard deviation of SMOS background departures over sea at 50° incidence angle, V polarisation covering 1st September 2023 to 31st August 2024.

2.4. Scatter plots

In the scatter plots statistics are accumulated from 1st September 2023 to 31st August 2024 and plotted as a 2-dimensional histogram with incidence angle on the x-axis and background departure on the y-axis. These plots allow the distributions of background departures at different incidence angles to be analysed.

Figure 9 shows that the distribution of background departures is centred close to zero for all incidence angle bins. It also shows that the histograms are close to symmetric, which can be seen by looking at the number of observations in the background departure bins with a similar magnitude but opposite signs. The distributions of background departures are very similar than in 2022/23 (Salonen et al., 2024a), except that the number of observations has decreased by nearly 18%. This is explained by the GPS anomaly (8th – 13th September 2023) and safe hold mode (22nd February – 12th March 2024) periods when no data was available (see Section3). In addition, more data is affected by RFI and thus screened out. The global mean background departures for each incidence angle bin are also close to zero although there are significant regional biases, see section 2.3.

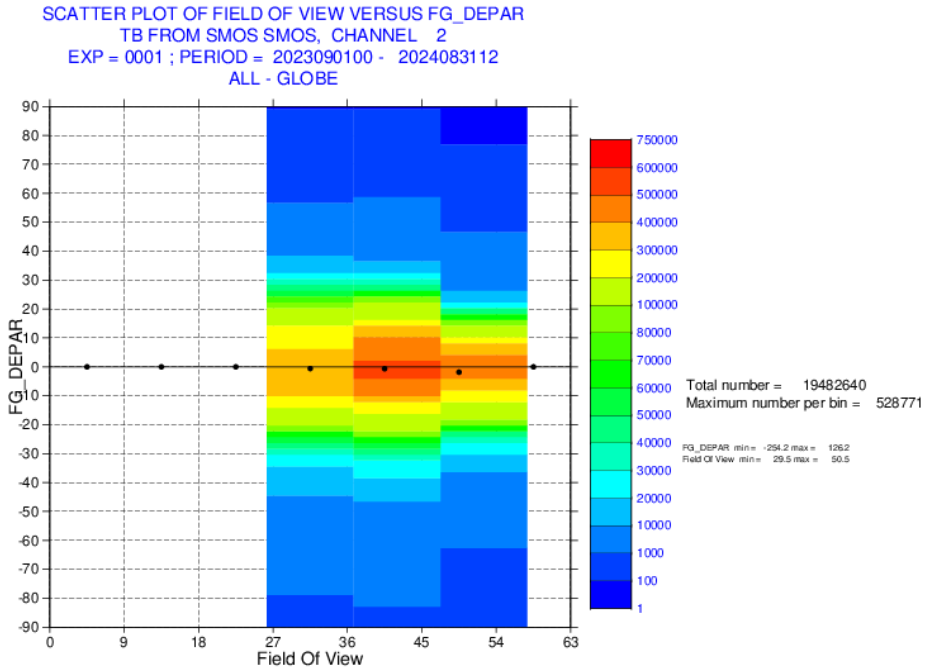

Figure 9: Scatter plot showing a 2D-histogram of SMOS background departures over land for different incidence angle bins, V polarization covering 1st September 2023 to 31st August 2024. The black dots represent the mean background departure for each incidence angle bin.

3. Notable features in 2023/24

This section describes notable features which are visible in the monitoring plots for September 2023 to August 2024.

3.1. GPS anomaly 8th – 13th September 2023

The time series and Hovmöller plots (Figures 1 – 5) show that there is no SMOS data in the statistics during 8th – 13th September 2023. The anomaly started 8th September 15:45:33 UTC when the value of the GPSOPSATUS triggered to 'nosat'. This was due to the platform GPS anomaly which was likely caused by a GPS spoofing signal. The issue was fixed on 13th September when the data dissemination also returned. Figure 10 shows the timeseries of the global ECMWF monitoring statistics for SMOS brightness temperature, horizontal polarisation and incident angle 30°. Upper panel is the background departure standard deviation, middle panel the mean background departure and the lower panel number of observations. The monitoring statistics indicate that after the fix the quality of the observations returned back to the level where they were before the GPS anomaly occurred. Few suspicious quality observations were disseminated during the period as seen in Fig. 10 but these were filtered out from the yearly monitoring statistics for September 2023 – August 2024.

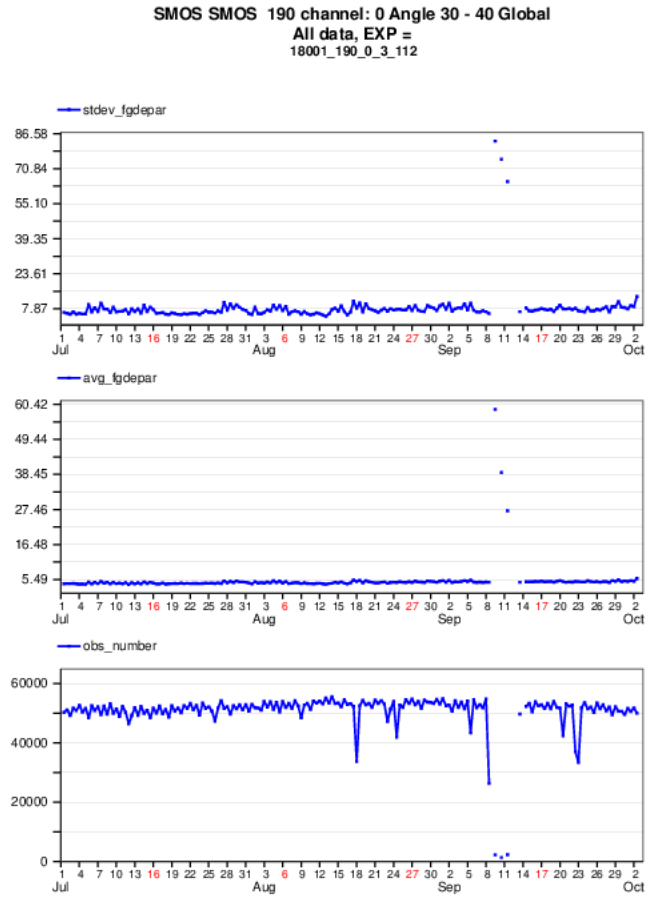

Figure 10. Time series of background departure standard deviation (upper panel), mean background departures (middle panel) and number of observations (lower panel) for H polarisation and incident angle 30°. Covered period is July 2023 – September 2023.

3.2. New RFI signal in Pacific Ocean 3rd October 2023

Figure 3 indicates that there are increased background departure differences on 3rd October 2023 over sea. Figure 5 further reveals that the anomaly in the statistics is spread from 15°S to 30°N. To investigate the feature in more details, Fig. 11 shows maps of the background departure standard deviation during 2nd - 4th October (upper panel) and 5th – 6th October 2023 (lower panel). There are two areas in the Pacific Ocean where the background departure differences are increased, namely a localised area in Central Pacific 0 - 10°N and a larger area 15°S to 30°N over Bay of Bengal, Indonesia and Philippine sea. The statistics have generally returned to normal levels after 3rd October and the sources, excluding over Bay of Bengal related to events in Myanmar, have not re-appeared since, so no further action in the investigations has been taken.

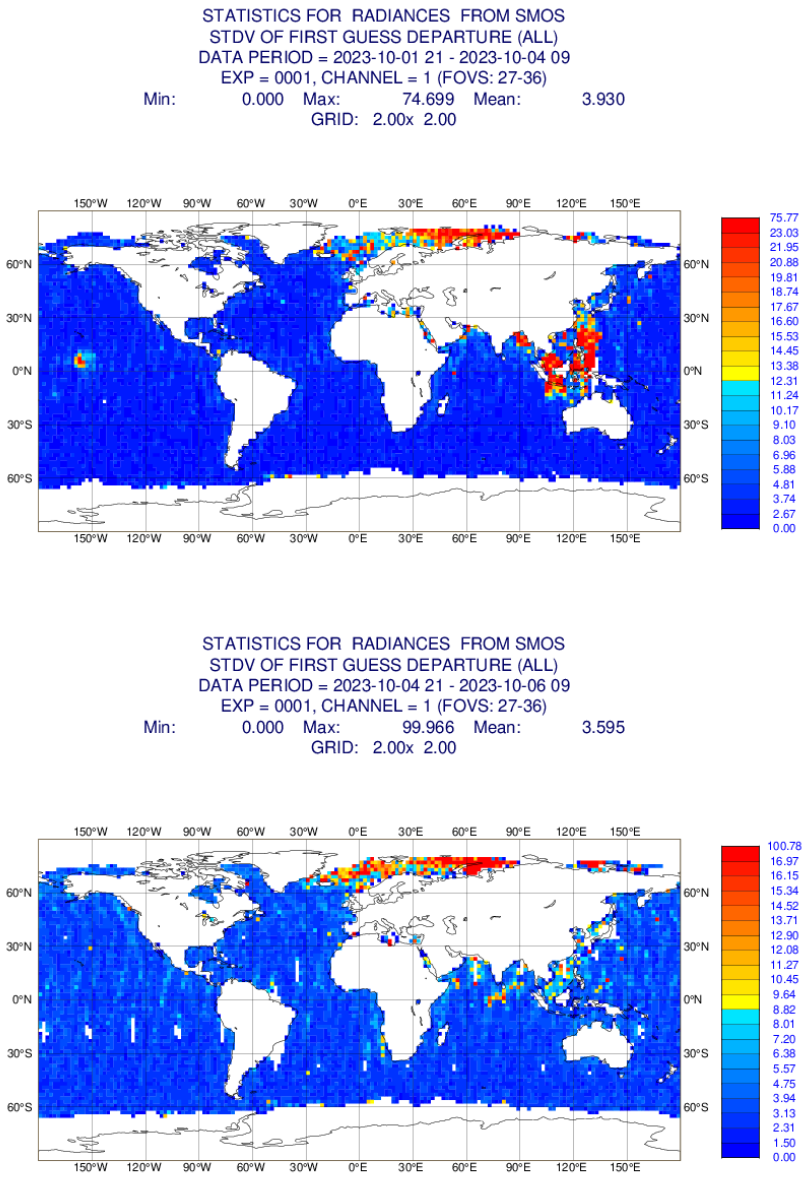

Figure 11. Maps of the background departure standard deviation during 2nd - 4th October 2023 (upper panel) and 5th – 6th October 2023 (lower panel) for H polarisation and incident angle 30°.

3.3. Anomaly over sea November 2023 – February 2024

The Hovmöller plots discussed in Section 2.2 in Fig. 5 are showing an increase in the observation and background departure standard deviations over sea surfaces from November 2023 to February 2024 between 0 and 45°N. The increase in the standard deviation is clear, especially for incidence angle 30° but the magnitude is notably smaller than seen for the known RFI events. At the same time the number of observations is decreasing over Southern hemisphere. Similar anomalies occurred in winter 2021-22 and 2022-23 (Salonen et al., 2023) and have been explained by solar effect.

Figure 12 shows the background departure standard deviation for ascending (upper panel) and descending (lower panel) orbits. The anomaly is visible only in the descending orbit. During November 2023 – February 2024 the solar activity has been again very strong and the strong solar activity can impact the accuracy of the faraday rotation due to higher uncertainty in the total electron content in the atmosphere. In the ECMWF system, the quality control applied for SMOS brightness temperatures screens out observations where the solar reflection bit is set and these are not included to ODB files ingested by the model. The reduction in the number of observations seen in Fig. 5 is thus a consequence of the quality screening due to reflected sun. Despite the observations affected by solar effect are screened, the signal from the sun is spread on the entire snapshot and is seen as increased standard deviation of the observations and background departures. This is strong over the northern hemisphere where the sun is in front of the antenna. On the contrary, in the ascending passes the sun is in the back of the antenna and its impact is attenuated by the antenna patter and the statistics are more homogeneous.

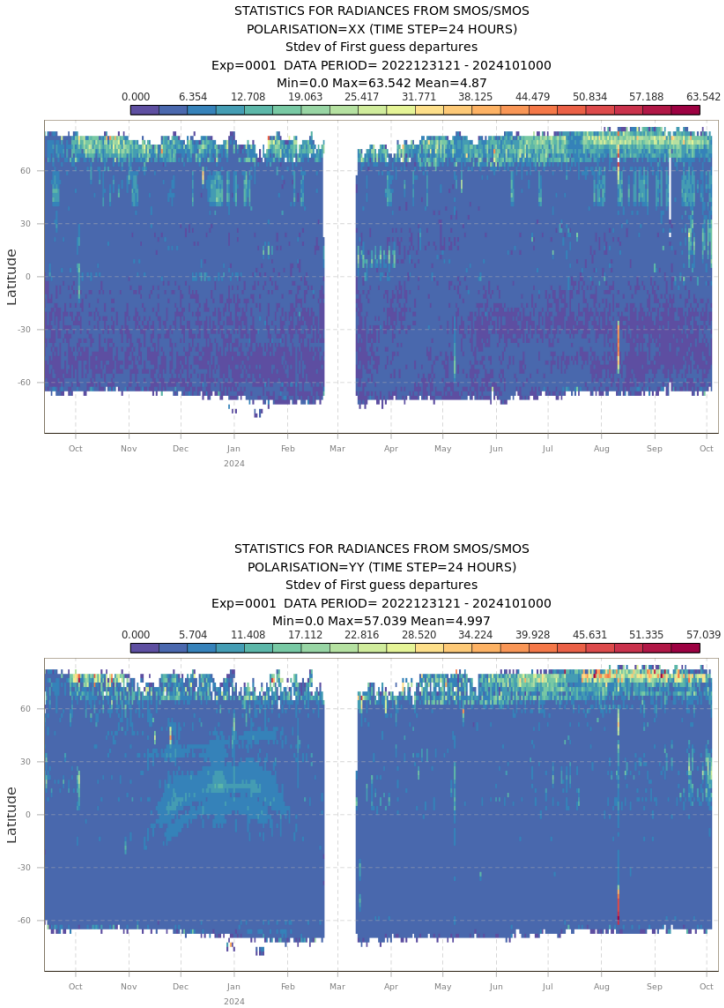

Figure 12. Hovmöller plots showing SMOS background departure standard deviation for ascending orbit (upper panel) and descending orbit (lower panel) over sea at H polarisation and 30° incidence angle.

3.4. Increased RFI signal over Bering Sea 14th December 2023 and 13th May 2024

Figure 3 shows an increase in the magnitude of the standard deviation of the background departures as well as of the observed values over sea on 14th December 2024. The Hovmöller plot in Fig. 5 further indicates that the increase is occurring between 55 - 65°N. Figure 13 shows a map of the background departure standard deviation for 12th – 15th December 2023. A new localized RFI signal is visible over the Bering sea. A similar anomaly over the same area is also observed on 13th May 2024 (not shown). However, it has not have not re-appeared, so no further action in the investigations has been taken.

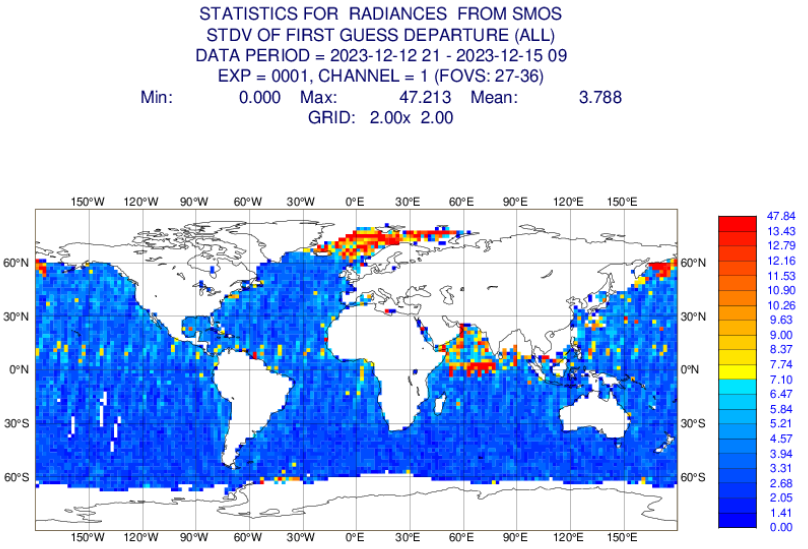

Figure 13. Map of the background departure standard deviation during 12th - 15th December 2023 for H polarisation and incident angle 30°.

3.5. New RFI signal south of Greenland 1st January 2024

Another spike in the background departure standard deviation is seen on 1st January 2024 in Fig. 3. This is related to a short lived RFI source south of Greenland over North Atlantic Ocean as illustrated in the map in Fig. 14. The RFI source has not re-appeared since, so no further action in the investigations has been taken.

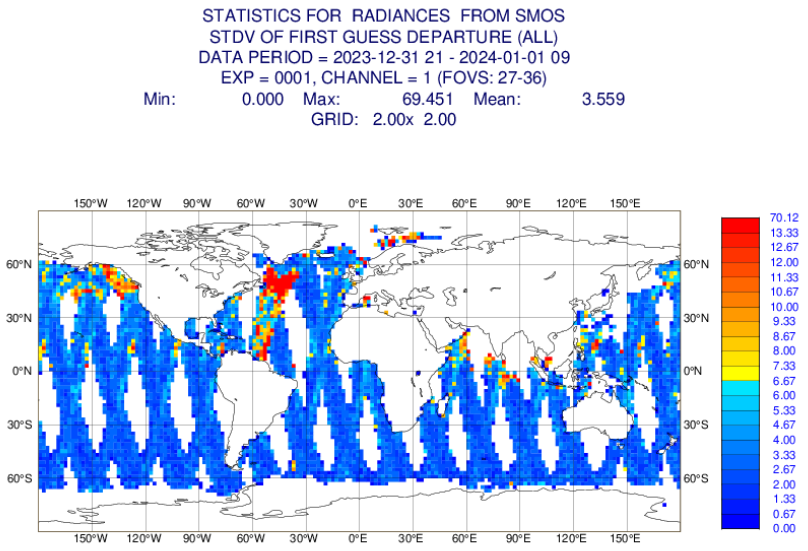

Figure 14. Map of the background departure standard deviation 1st January 2024 for H polarisation and incident angle 30°.

3.6. SMOS safe hold mode impacting data availability 22nd February – 12th March 2024

The timeseries and Hovmöller plots (Figures 1 – 5) indicate also a second extensive period with no SMOS data available in the 2023/24 monitoring period, namely 22nd February – 12th March 2024. Reason for the outage is that SMOS experienced an anomaly and entered safe hold mode on 22nd February 5:10 UTC. The anomaly was triggered by a platform fault detection related to a platform on board software data corruption which was likely caused by a radiation single-event upset (SEU). The MIRAS instrument was successfully activated on 27th February and the science operations were resumed but the data was not disseminated to the end-users while data quality was under investigations. Unexpectedly SMOS entered safe hold mode again on 3rd March 15:59 UTC. The reason seemed similar to the first incident. The investigations after the first safe hold mode indicated that the anomaly was related to the PM-A unit and thus, it was decided to recover the MIRAS instrument on the PM-B unit. The platform swich-on was completed on 6th March followed by the payload switch-on on 7th March 2024. The quality checks indicated that the platform and the MIRAS instrument were operating as expected and the data dissemination was resumed on 12th March 2024.

Figure 15 shows the global ECMWF monitoring statistics for SMOS brightness temperature over land, horizontal polarisation and incident angle 30 for 1st February – 25th April 2024. Upper panel is the background departure standard deviation, middle panel the mean background departure and the lower panel number of observations. The monitoring statistics indicate that after the data dissemination was resumed the background departure standard deviation had an increasing trend. Further investigations indicate that the increase in the standard deviation originates from the Tropics and more specific from south of the Arabian Peninsula where a strong RFI pattern has not been fully removed by the RFI screening as illustrated in Fig 16. Thus, the increase in the OmB standard deviation after the data dissemination was resumed is unrelated to the SMOS safe hold mode period.

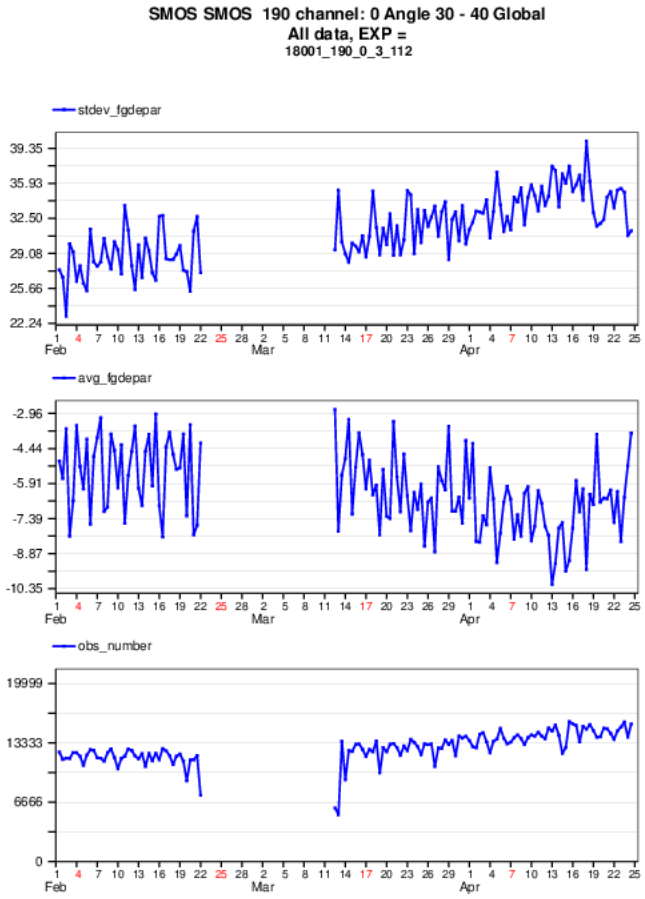

Figure 15. Time series of background departure standard deviation (upper panel), mean background departures (middle panel) and number of observations (lower panel) for H polarisation and incident angle 30° over land. Covered period is February – April 2024.

3.7. Increased observation and background departure standard deviations on 8th May 2024

Figure 5 indicates increase in the magnitude of standard deviation both for observed values and for background departures on 8th May 2024 and the increase is wide spread, from 60°S to 40°N. Figure 17 shows the map of the background departure standard deviations on 8th May for H polarisation and incident angle 30° and indicates that there are 2-3 orbits with the affected statistics. On 8th May several strong Solar Radio Burst (SRB) have been detected, contaminating the retrieved Brightness Temperature. On May 8th data from 0748z to 1021z are affected by anomalous Chi-2 and lack of sea surface salinity retrievals and on May 9th data from 0849z to 0939z are also impacted on the same way. (R. Crapolicchio, personal communication).

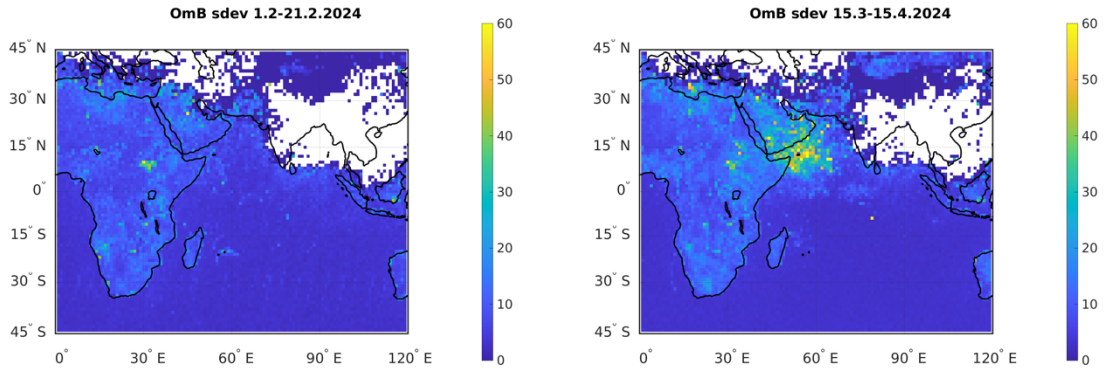

Figure 16: Maps of background departure standard deviation for 1st – 21st February 2024 (left panel) and 15th March – 15th April 2024. The SMOS brightness temperatures are RFI screened, horizontal polarisation and incident angle 30°.

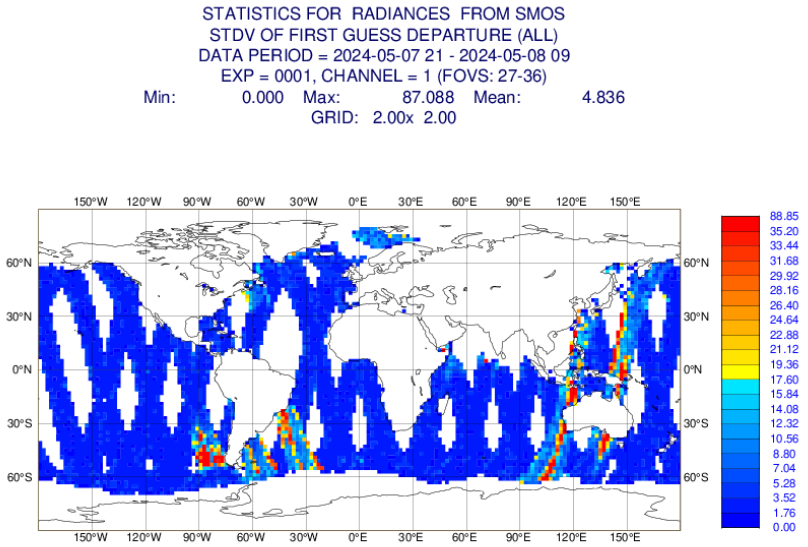

Figure 17. Map of the background departure standard deviation 8th May 2024 for H polarisation and incident angle 30°.

3.8. New RFI source 11th August 2024

A third gap with no data in the time series and Hovmöller plots presented in Section 2 is 11th August 2024. This was excluded as the statistics for the day, especially over land, where increased significantly and made other events occurring during the monitoring period not to stand out. Figure 18 shows the timeseries plot over land during 10th – 12th August for H polarisation and incident angle 30°. The

timeseries reveals that anomaly affects the statistics during 09 – 21 UTC on 11th August. There is significant drop in the background departure mean, due to a drop in the observation value, and increase in the background departure standard deviation. Figure 19 shows the map of the background departure standard deviations for the same period and indicates that the observation anomaly originates from Alaska.

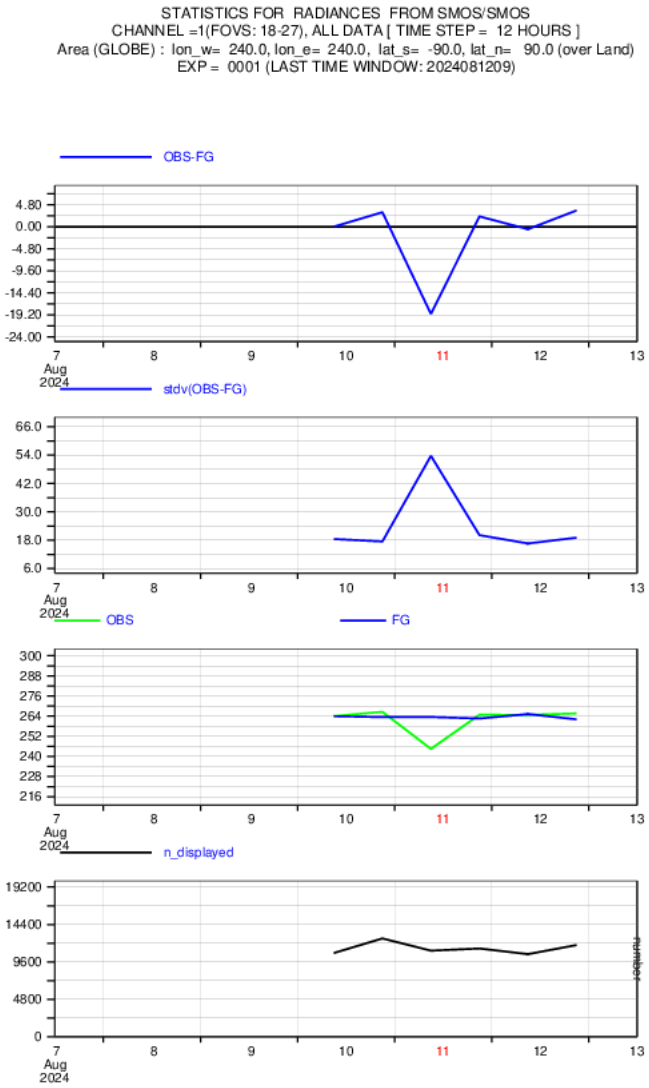

Figure 18: Time series of mean background departures (upper panel), standard deviation of background departures (2nd panel), mean observed and background values (3rd panel) and number of observations (lower panel) over land at 30° incidence angle, H polarisation and cover 10th – 12th August 2024.

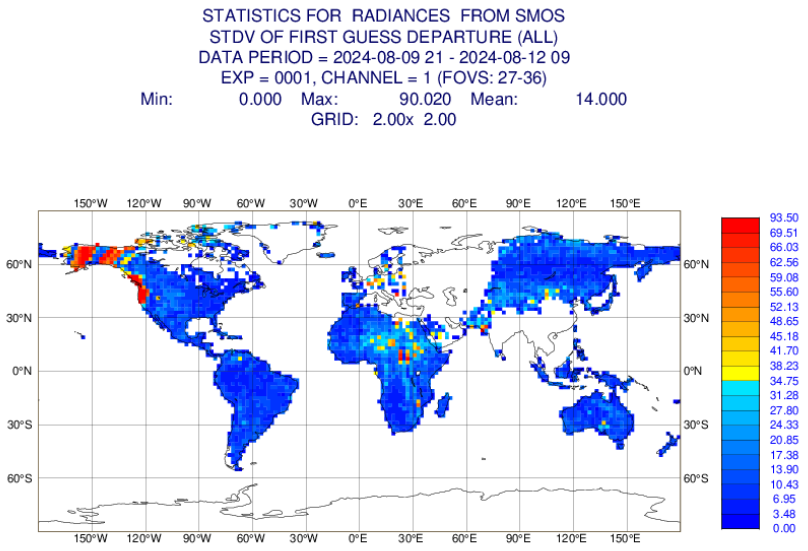

Figure 19. Map of the background departure standard deviation 10th -12th August 2024 for H polarisation and incident angle 30°.

4. Comparisons to SMAP

Since 11th May 2021 the monitoring of the NASA Soil Moisture Active Passive (SMAP) instrument has also been part of the ECMWF operational system, using the same framework as the SMOS monitoring. SMAP was launched in 2015 and the instrument measures at L-band (1.41GHz) the same frequency as SMOS and therefore comparisons between the monitoring statistics for SMOS and SMAP are very relevant for unpicking observation and model issues in the background departures.

The comparisons presented in section 4.1 were made with data from September 2023 to August 2024 with the v724 SMOS L1 Tbs and most up-to-date SMAP Tbs in the operational system. The SMOS observations used in the comparison are limited to those with incidence angles between 39.5° and 40.5° which best match the 40° incidence angles of the SMAP observations. Also, the operational screening including the most up-to-date RFI screening is applied to the SMOS data. By contrast, SMAP has onboard RFI screening which is applied to the data before it arrives at ECMWF. CMEM with the same settings is used as the observation operator or both the SMOS and SMAP observations.

4.1. September 2023 to August 2024 comparison

Figure 20 shows that the standard deviation of background departures is slightly smaller for SMAP than for SMOS for V polarisation. For H polaristion the magnitudes are more similar (not shown). The SMAP mean background departures are more negatively biased with the magnitude of bias larger than for SMOS. Despite these small differences between SMOS and SMAP, the statistics are largely comparable and the results agree with comparisons made previously in Weston and de Rosnay (2022)

and Salonen et al., 2024a. There is data outage for SMAP December 2023 – mid January 2024, the reason for this is unknown.

Figure 21 shows that the gridded standard deviation values of background departures are significantly smaller for SMAP than they are for SMOS with the largest differences in Asia, the middle East and South-Eastern Europe, all areas where there are significant RFI sources. This indicates that the onboard screening for SMAP is still doing a better job than the v724 SMOS screening. The differences shown figure 21 for 2023-2024 are larger than reported in Salonen 2024a for 2022-2023. This result is consistent with increased RFI sources over land in the last 12 months as discussed in Section 2.3. In addition, over areas not affected by RFI, the SMAP standard deviation of background departures are also smaller than for SMOS albeit to a slightly lesser degree. This indicates that SMAP has lower instrument noise than SMOS which is expected because the SMOS instrument was designed to reduce the noise by averaging over different incidence angles. In this analysis only a small range of SMOS incidence angles are used so there is no reduction in noise from the use of multiple incidence angles.

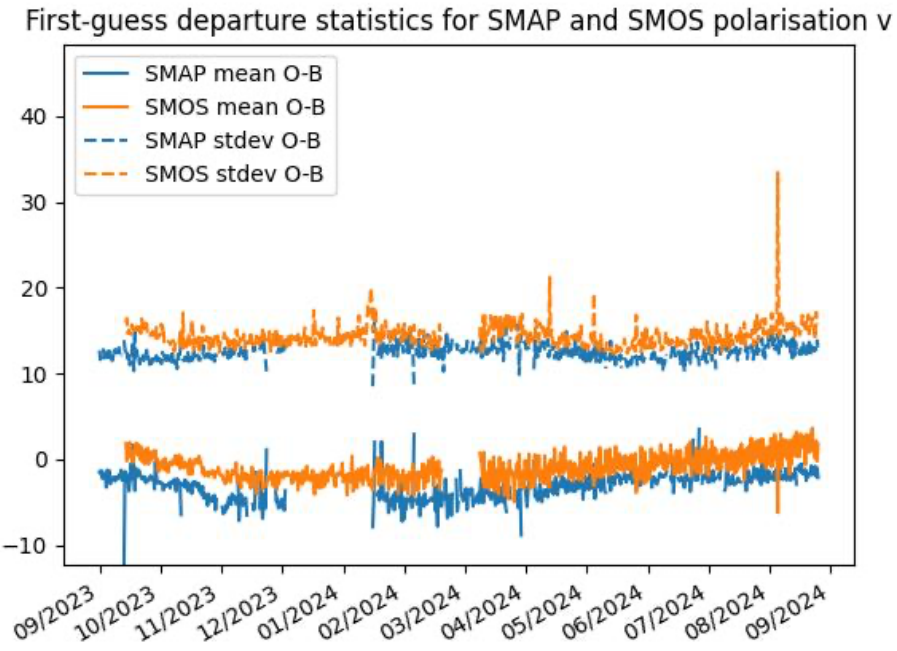

Figure 20: Time series of mean (solid lines) and standard deviation (dashed lines) of background departures for SMAP (blue) and SMOS (orange) for V polarisation between 1st September 2023 and 31st August 2024.

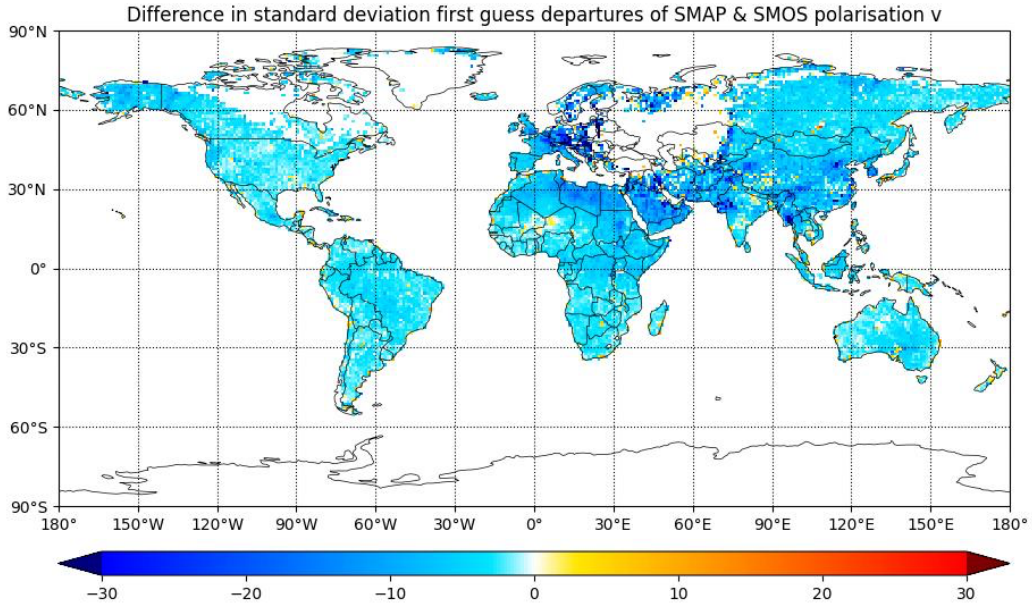

Figure 21: Difference in gridded standard deviation of background departures for V polarisation between SMAP and SMOS. Statistics are calculated between 1st September 2023 and 31st August 2024

5. Future enhancements to the monitoring system

5.1. Bias correction

An adaptive soil moisture bias correction scheme is under development for future implementation in the IFS in the next couple of years. It will complement the current CDF-matching approach which is used for soil moisture data assimilation into the simplified extended Kalman filter (SEKF). Applying this approach to the SMOS Tbs could be investigated in the future to improve on the results shown in section 3.3 and will be relevant for future assimilation experiments too.

5.2. Observation operator and model enhancements

As alluded to in section 2.1 , sub-optimalities in the observation operator are one of the potential sources of the residual biases in the SMOS background departures. As part of a new Horizon Europe project called CERISE (CopErnIcus Climate change Service Evolution), that started in January 2023, there will be work to enhance the observation operator for low frequency microwave observations in general (including at L-band frequencies) using machine learning approaches. This is expected to lead to improved performance leading to smaller biases in the SMOS background departures in the future. The timescale on this project is that the newly developed observation operator should be available in 2025.

Furthermore, developments in the ECMWF land surface model are ongoing to investigate the potential of a finer vertical discretization in the soil. This development is highly relevant to better represent the

top-layers soil moisture dynamics, with expected potential improvements in model forward modelling capabilities. Machine learning approaches will be investigated to explore SMOS brightness temperature forward modelling using a multi-layer soil moisture approach.

References

de Rosnay, P., J. Muñoz-Sabater, C. Albergel, L. Isaksen, S. English, M. Drusch, J.-P. Wigneron: SMOS brightness temperature forward modelling and long term monitoring at ECMWF. Remote Sens. Environ., 237 (2020): 111424. https://doi.org/10.1016/j.rse.2019.111424

Liu, Q., Weng, F., and English, S.: An improved fast microwave water emissivity model, IEEE, T. Geosci. Remote, 49, 1238–1250, 2011.

Salonen K., P. Weston, P. de Rosnay: "Annual SMOS brightness temperature monitoring report", ESA SMOS ESL contract 4000130567/20/I-BG, February 2024 doi:10.21957/64e9d1fcec, 2024a

Salonen, K., Weston, P., and de Rosnay, P.: Quality control plan for brightness temperature monitoring - 2024. ESA contract report. SMOS ESL contract 4000130567/20/I-BG, 2024b

Saunders, R., Hocking, J., Turner, E., Rayer, P., Rundle, D., Brunel, P., Vidot, J., Roquet, P., Matricardi, M., Geer, A., Bormann, N., and Lupu, C.: An update on the RTTOV fast radiative transfer model (currently at version 12), Geosci. Model Dev., 11, 2717–2737, https://doi.org/10.5194/gmd-11-2717-2018, 2018.

Weston, P., P. de Rosnay: Annual SMOS brightness temperature monitoring report - 2021/22. ESA contract report. SMOS ESL contract 4000130567/20/I-BG, December 2022b

Weston and de Rosnay; SMOS brightness temperature monitoring quality control review and enhancements, *13*(20), 4081, Remote Sensing, 2021 https://doi.org/10.3390/rs13204081